Binding energy correction to the kinematics of quasifree scattering

P. C. Gugelot*
Max-Planck-Institut für Kernphysik, Heidelberg, Federal Republic of Germany
(Received 10 November 1983)

A model is developed which accounts for the observed momentum shift of 10—50 MeV/c between experimental results and distorted wave impulse approximations. Kinematical effects of the binding energy and the Fermi momentum in reactions of the type $A(x,yz)B$ are considered to be responsible for the shift. Several examples are discussed.

I. INTRODUCTION

Medium and high energy nuclear reactions are often analyzed by a "quasifree" scattering approximation. An incoming particle interacts only with a nucleon or with a substructure of the target nucleus. The remaining part of the target nucleus remains a spectator. Such reactions are of the type (p,2p) (Ref. 1), $(\alpha,p\alpha)$, and many others. In general, we may designate these reactions by $A(x,yz)B$, in which the residual nucleus B is the spectator. The projectile x interacts with a fragment of A, $(A-B)$ initiating the reaction $x+(A-B)\rightarrow y+z$. This approximation is assumed to be applicable when the de Broglie wavelength of the projectile is small compared to the internuclear distances. In first approximation, plane waves for the incoming and outgoing particles are used. The introduction of distortions or of rescattering will improve the fits. The second order approximation decreases the cross section in the region of small momentum transfer by as much as an order of magnitude. The plane wave solutions will not satisfy without additional assumptions the required orthogonality between initial and final states.[2]

In the elementary treatment of quasifree scattering one assumes that neither the incident particle nor the interacting fragment or the spectator suffers from any binding forces. Not only is the free scattering matrix used, but also the kinematical effects due to the binding are neglected. In more realistic treatments the binding is considered in a bound transition matrix.[3] In addition, multiple scattering processes have to be taken into account inside the nuclear medium, especially in those cases when the incoming particle is strongly interacting. This applies for pions in the 3,3 resonance region[4] in particular.

Thies[5] calculated the quasielastic pion scattering on ^{16}O and compared his results to the Schweizerisches Institut für Nuklearforschung (SIN) experiment by Ingram *et al.*[6] He uses essentially a distorted-wave impulse approximation (DWIA). The incoming pion interacts with a nucleon, forms a Δ which propagates through the nuclear matter. The optical potential for the distortions is generated by the t operator which also produces the transitions. The T matrix is evaluated at the value of the final nucleon momentum. A shift in the position of the quasielastic peak as a function of incident energy and scattering angle is attributed to a change of the kinetic energy operator for the Δ. Above resonance, the quasielastic peak is shifted towards larger energy losses, below resonance towards smaller ones. The calculated values for ^{16}O are at 130° pion angle

18 MeV at 240 MeV ,

-11 MeV at 115 MeV ,

in approximate agreement with the experiments.[6] However, unfortunately, the experimental points around the peak are missing such that a precise determination of the peak position cannot be made.

The case discussed here is complicated due to the pion-nucleon resonance. Even though this calculation takes many aspects of the interaction into account a *kinematically* induced shift due to the binding of a proton to the nitrogen core has not been considered.

Chrien *et al.*[7] observed the quasielastic scattering of 800 MeV protons from different nuclei at several angles. Figure 1 shows the experimental points for carbon and the results of a DWIA calculation. The peak position is off by 22 MeV/c. Such a shift has been observed in numerous experiments and it is generally believed to be caused by the binding energy.[8] In this paper we develop a simple kinematical model which accounts for the shift in Fig. 1 and has been successfully applied to many experiments.

One can easily show how the shift comes about by considering an interaction in the longitudinal direction. Let a particle be bound with an energy Q in a potential hole. A

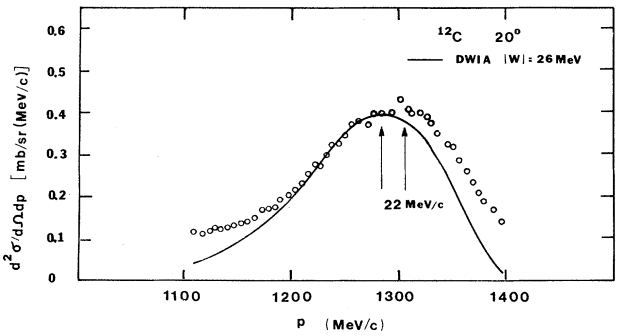

FIG. 1. The experimental points for 800 MeV protons scattered from carbon and the results of a distorted wave calculation (Ref. 7). The shift of the peak of 22 MeV/c is predicted by the model presented here.

projectile of mass m_1 and momentum p_1 enters the potential to collide with the bound particle. Upon entering, the projectile causes the potential to recoil with momentum $p_r = m_1 Q/p_1$. After the collision the changes of momentum of the two particles due to their emerging from the potential cancel and, therefore, they do not contribute to an additional recoil momentum. The potential still recoils with momentum p_r and this p_r has to be subtracted from the momentum of the projectile. It corresponds to the shift observed in experimental momentum distributions.

Using the basic idea given above we will discuss the interaction in more precise terms. Figures 2(a) and (b) represent the interaction. Figure 2(a) deals schematically with the breaking up of the target of mass m_2. The bubble signifies the energy and the momentum which is taken from the incoming particle to produce the recoil as described above. Figure 2(b) presents the diagram of the complete interaction. The upper vertex is the quasifree reaction $m_1 + m_q \rightarrow m_3 + m_4$. To dissociate the target, m_1 has to lose energy ϵ and momentum $\Delta\vec{p}$ in the z direction. According to our naive model $\Delta\vec{p}$ is in the direction of $\vec{p}_1$.

T_1, p_1 and T_0, p_0 are the kinetic energy and momentum of the incident particle before and after the dissociation of the target. Then $\Delta p = p_1 - p_0$ and $\epsilon = T_1 - T_0$. The dissociation energy ϵ includes the Fermi energy which the fragments may possess. Solving for Δp and expanding the square root we obtain

$$\Delta p \approx \frac{m_1}{p_1}\epsilon \,. \tag{1}$$

The momentum Δp is taken up by the target m_2. It is the recoil momentum of m_2 as has been discussed above. Consequently, the momenta $\vec{q}$ and $\vec{p}_5$ of the fragments which are diametrically opposed in the frame of the recoiling target are not so anymore in the laboratory frame. In the recoiling frame, $\vec{q}\,' + \vec{p}\,'_5 = 0$. The primes denote the recoiling frame. The velocity of that frame is $v_r = \Delta p/m_2$ in the z direction, $\vec{v}_r = v_r \hat{k}$. The relations for the momenta of the fragments in the recoiling and in the laboratory frame are

$$\vec{q} = \vec{q}\,' + m_q \vec{v}_r \tag{2a}$$

and

$$\vec{p}_5 = \vec{p}\,'_5 + m_5 \vec{v}_r \tag{2b}$$

for the energy in the laboratory frame, and

$$q^2/2m_q + p_5^2/2m_5 = \epsilon + Q \,, \tag{2c}$$

in which Q is the binding energy. Expressing the laboratory momenta $\vec{q}$ and $\vec{p}_5$ in terms of the momenta in the recoiling frame in which the Fermi momentum actually is defined and expanding the square roots again, we find,

$$\epsilon = \frac{m_q + m_5}{m_q m_5}\frac{q'^2}{2} - Q \,, \tag{3}$$

$$\Delta p = \frac{m_1}{p_1}\left[\frac{m_q + m_5}{m_p m_5}\frac{q'^2}{2} - Q\right] . \tag{4}$$

The change of momentum is just what the naive model predicted. In addition, however, the Fermi momentum which m_q may possess in the frame of the target nucleus is taken into account. The shift in momentum is equal to the binding energy Q over the velocity of the projectile. Abul-Magd, Hüfner, and Schürmann also obtained this result with different reasoning.[9]

The calculation of the upper vertex interaction can now proceed as in a normal two-body interaction with the incoming momenta p_0 and q. In the impulse approximation, the off-shell interaction is replaced by an on-shell reaction, in contrast to other calculations for which the amplitudes are taken at the "half-shell."[10] For symmetrical emission of particles 3 and 4, the center of mass angle in the upper vertex is 90°.

In Sec. II we will discuss the complete relativistic kinematics to calculate p_0 and q and discuss some examples of the shift in the momentum spectra. In Sec. IV a complete calculation for the quasifree elastic scattering of 5 GeV/c pions on ^{4}He will be presented.

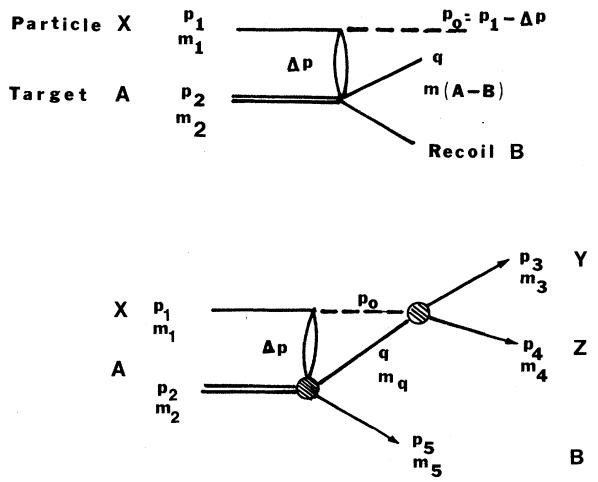

FIG. 2. The reaction $A(x,yz)B$ is represented. In (a), the incoming particle x with four-momentum p_1 and mass m_1 collides with the target nucleus A which is dissociated into m_q and the recoiling nucleus B. The projectile loses four-momentum Δp in this process. In (b), the complete reaction is schematically shown. The upper vertex, the collision between m_1 and m_q, is now on shell.

II. KINEMATICS

The relativistic kinematics of the reaction $A(x,yz)B$ will now be discussed. The same model is used. As shown before it presents a procedure for the construction of an expression for the momenta p_0 and q as a function of the binding energy Q and the Fermi momentum q' of m_q and m_5. Figures 2(a) and (b) illustrate the interaction. In the primed target nucleus, or recoiling frame, the fragments satisfy the condition

$$\vec{q}\,' + \vec{p}\,'_5 = 0 \,. \tag{5}$$

The Fermi momentum is one set of variables which describes the reaction. It is practical to call the reaction plane that which is determined by the incoming momen-

tum $\vec{p}_1=p_{1z}$ and by $\vec{q}$. The angle θ_F is between $\vec{q}$ and $\vec{p}_1$. Figure 3(a) shows the coordinate system and Fig. 3(b) indicates the target nucleus which is fragmented into m_q and m_5. The incoming particle gave up energy $\epsilon=E_1-E_0$ and three-momentum in the z direction $\Delta p=p_1-p_0$. The momentum p_0 and total energy E_0 still satisfy $E_0^2-p_0^2=m_1^2$. At any instant, energy and momentum will remain conserved. In a four-vector notation we have

$$p_{\text{in}}=p_1+p_2=p_0+q+p_5 \ , \tag{6}$$

and for the upper vertex,

$$p_0+q=p_3+p_4 \ . \tag{7}$$

Condition (5) requires a nuclear frame, the recoiling target nucleus, which moves in the laboratory. This condition is sufficient for the determination of the velocity $\vec{B}$ of the nuclear frame moving in the z direction. The four-vectors satisfy the following relations:

$$(p_{\text{in}}-p_0)^2=(q+p_5)^2=(q'+p_5')^2 \ , \tag{8}$$

$$p_{\text{in}}=p_1+p_2 \ . \tag{9}$$

The Fermi momentum q' is a variable of the reaction and we can solve for the three-momentum p_0 in terms of the Fermi energy $E_q'=(q'^2+m_q^2)^{1/2}$ and $E_5'=(q'^2+m_5^2)^{1/2}$,

$$p_0=\frac{1}{s}[p_1M^2+E_{\text{in}}(M^4-m_1^2s)^{1/2}] \ , \tag{10}$$

$$M^2=0.5[s+m_1^2-(E_q'+E_5')^2] \ . \tag{11}$$

One can express p_0 also in terms of experimental quantities from Eq. (6),

$$\begin{aligned} &p_0=(\mu(p_{\text{in}}-p_5\cos\theta_5)+E_{34}\{\mu^2-m_1^2[E_{34}^2-(p_1-p_5\cos\theta_5)^2]\}^{1/2})/[E_{34}^2-(p_1-p_5\cos\theta_5)^2] \ , \\ &\mu=\tfrac{1}{2}(m_q^2-s-m_1^2-m_5^2-2p_1p_5\cos\theta_5+2E_{\text{in}}E_5) \ , \\ &E_{34}=E_{\text{in}}-E_5=E_3+E_4 \ . \end{aligned} \tag{12}$$

It is now necessary to calculate the velocity of the nuclear frame B, which determines $\vec{q}$ and $\vec{p}_5$ in the laboratory. The invariant squared energy s expressed in the moving system is

$$s=(p_0'+q'+p_5')^2=(p_1+p_2)^2 \ . \tag{13}$$

Equation (13) determines p_0', i.e., the momentum of m_1 after the target nucleus is dissociated in the frame of the target nucleus. The energy of p_0' is

$$E_0'=\frac{s-(E_q'+E_5')^2-m_1^2}{2(E_q'+E_5')} \ , \tag{14}$$

and three-momentum,

$$p_0'=(E_0'^2-m_1^2)^{1/2} \ , \tag{15}$$

since m_1 remains on shell. As in Eq. (11), $E_q'+E_5'$ is the total Fermi energy in the moving nuclear frame. The vectors $\vec{p}_1$ and $\vec{p}_0$ are always in the z direction of the coordinate system. Therefore, we write them as scalars.

The velocity of the nuclear frame is the difference of the velocities of p_0 in the laboratory and, in the recoiling frame

$$B_z=\frac{p_0E_0'-p_0'E_0}{E_0E_0'-p_0p_0'} \ . \tag{16}$$

Finally, a Lorentz transformation will transform the momenta and energy of p_5' and q' into the laboratory system.[11]

$$\vec{p}_5=\vec{p}_5'+\vec{B}\gamma\left[\frac{\gamma}{\gamma+1}\vec{B}\cdot\vec{p}_5'+E_5'\right] \ , \tag{17}$$

$$\gamma=(1-B^2)^{-1/2} \text{ and analogous for } q' \ . \tag{18}$$

It can be shown that for $p_1/E_1 \ll c$ the results of the relativistic expressions are equal to those derived in the Introduction.

The remaining kinematics for the upper vertex is now a straightforward two-body interaction which takes place on the mass shell, in four-vectors,

$$p_0+q\rightarrow p_3+p_4 \ . \tag{19}$$

Equation (19) shows that the upper vertex is dependent on the Fermi momentum through q *and* p_0. In the regular impulse approximation p_0 corresponds to the incoming momentum and the vertex is dependent on q only. Here,

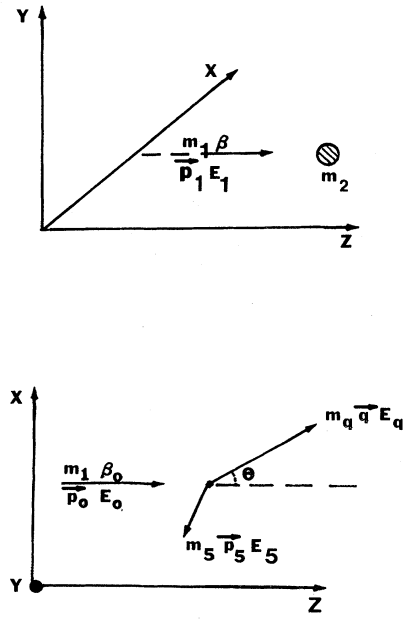

FIG. 3. The coordinate system used in the calculation. The target A of mass m_2 dissociates into m_q and m_5. The fragments have three-momentum q and p_5, respectively. These define the x-z plane.

for reaction (19) the three-momentum p_0 and the energy E_0 of m_1 decrease with increasing Fermi momentum. As a consequence, the momentum transfer in (19) is not as large as the momentum transfer between p_1 and p_3. It is here that the ordinary impulse approximation will require Fermi momenta larger by as much as 100 MeV/c to explain the observed large momentum transfers between p_1 and p_3. In addition, the momentum distribution will not be symmetric around $q=0$. This model limits the maximum possible Fermi energy. Namely, p_0 has no real solution if

$$\frac{m_1(m_1+m_2)}{M^2}>1 . \tag{20}$$

Or, one cannot borrow more energy from the projectile than its kinetic energy. This is not a limitation in the kinematics. However, it forbids reactions in which a virtual subthreshold particle m_q mediates the reaction such that the kinematic energy of m_1 is not sufficient to produce m_q and m_5 from the target m_2. At medium energies at which these approximations can be used the above is rarely a limitation. Other consequences of this model will be a shift observed in the quasifree scattering of a resonance for m_q and m_5, away from the free particle resonance.

In general, the interaction at the upper vertex will produce the particles m_3 and m_4 which are not in the reaction plane xz of Fig. 3(b). However, if m_q has spin 0 or spin $\frac{1}{2}$ the final products will remain in the xz plane.[12] This makes possible an experimental check whether or not the reaction proceeds according to the diagram.

III. MOMENTA SPECTRA

Two types of experiments are suitable for the quasifree scattering analysis, these are inclusive and exclusive reactions. In the former, one arm experiments, only the kinematics of one particle are determined. A very large number of such experiments exist. Out of space considerations we will discuss only some examples, though the model has been tested on many other experimental results.

It is assumed that the incident particle collides with one nucleon, either a proton or a neutron. In a one arm experiment the Fermi momentum of that nucleon cannot be determined explicitly. The resulting momentum distribution of the scattered particle is a function of the density distribution of nucleons, $\rho(q')$. That density distribution will have a maximum at the Fermi momentum $q'=0$ as long as a particular shell cannot be singled out.

Chrien *et al.*[7] measured the quasielastic scattering of 800 MeV protons from different elements. These authors analyzed the data by a DWIA calculation. Figure 1 shows a momentum shift of 22 MeV/c for the peak of the distribution for ^{12}C. All impulse approximation results have similar shifts. In Table I we present their observed peak positions and the ones obtained in our calculations for which $q'=0$ MeV/c is assumed. The agreement is good. Only some representative data are shown, all others fit as well.

Other hadron incident experiments have shown equally good agreement. Bunker *et al.*[13] observed a shift of about

TABLE I. Quasielastic scattering of 800 MeV protons (Ref. 7).

Target	Angle (deg)	Experimental peak position (GeV/c)	Calculated peak position (GeV/c)
^{6}Li	13	1.39	1.3878
	15	1.37	1.3757
	20	1.30	1.3096
	30	1.14	1.1398
^{7}Li	11	1.415	1.4122
	30	1.113	1.1433
Ca	11	1.41	1.4086
	15	1.37	1.3655
Pb	15	1.37	1.3705
	20	1.31	1.3064

10 MeV/c between the experimental data and the results of a plane-wave impulse approximation (PWIA) calculation. We predict a shift of 12.7 MeV/c. A similar result is obtained for the reactions ^{6}Li(p,pα) and ^{6}Li(α,2α) at 64.3 MeV as observed by Jain *et al.*[14] who shift their curves by 5 MeV/c. In this case we predict 2 MeV/c. Recently, the quasifree scattering of pions from ^{3}He and ^{4}He with incident energy between 300 and 475 MeV has been measured. At 60° the experimentally observed peak position agrees with the prediction. At larger angles, 90° and 120°, no pronounced quasielastic peak is found.[15] The experimental results of pions scattered from ^{16}O in the resonance region[6] are a special case. Since the cross section for the pion nucleon cross section changes rapidly one may not obtain the peak position in the quasielastic scattering at zero Fermi momentum. A small Fermi momentum ($q=0.05$ GeV/c) such that the total incident momentum for the upper vertex is $p_0\pm q$ will give complete agreement. The upper sign occurs when p_0 is below the resonance, the minus sign above the resonance. This makes the cross section for the upper vertex larger than for $q=0$, whereas the nucleon density for such a small q is still almost maximal.

Three-body final state reactions in which the full kinematics are measured can be used for the determination of the internal parameters, which for this model are the Fermi momentum and the kinematics of the scattering vertex. In principle, the equations given above can be inverted such that q and the scattering angle of the upper vertex can be determined from the values of p_3, p_4, and p_5.

Of the recent p,2p experiments with good energy resolution the data published by Frankel *et al.*[16] have been analyzed. For 0.8 GeV protons incident on ^{6}Li, a backward proton at 150° of momentum 0.35 and 0.4 GeV/c was detected and a forward proton with 1.35 and 1.32 GeV/c. The cross section peaked at about 16° and at 18°, respectively. From this result, for which, of course, energy and momenta are satisfied, one can deduce that the peak in the cross section corresponds to a proton recoiling

and a ^{5}He collides with the incident proton. Since the momentum and angle of the backward proton are known, one can determine the Fermi momentum of the ^{5}He substructure of ^{6}Li. Weber and Miller proposed such reactions.[17]

An inclusive experiment by the same authors,[16] detecting the forward protons only, showed peaks in the cross section at approximately the same angle as for the coincidence measurements. These results can be explained by a Fermi momentum $q'=0$ and a recoiling ^{5}He. At $\theta_p=16°$ the proton momentum is $p_3=1.356$ GeV/c, and at $\theta_p=18°$, $p_3=1.329$ GeV/c, in good agreement with the experiment.

IV. THE 5 GeV/c ^{4}He$(\pi^-,\pi^-\mathrm{p})^3$H REACTION

At CERN the reaction $^4\mathrm{He}(\pi^-,\pi^-\mathrm{p})^3\mathrm{H}$ at small momentum transfer has been studied. The particles were identified and the full kinematics was measured.[18] Chevallier *et al.*[19] and Fäldt[20] calculated the quasifree pion scattering cross section by making use of several diagrams and they obtained fairly good agreement with experiments. In this section we would like to recalculate the cross section on the basis of the present model. We will not introduce any free parameters and use the same density distribution as in the work of Fäldt.[20]

The cross section for two incoming spinless particles and a final state of one spinless and two spin $\frac{1}{2}$ particles is

$$\sigma=\frac{1}{|v_1-v_2|}\int\sum|T|^2\frac{d^3p_3}{(2\pi)^3 2E_3}\frac{m_4 d^3p_4}{(2\pi)^3 E_4}\frac{m_5 d^3p_5}{(2\pi)^3 E_5}\times\frac{(2\pi)^4}{2E_1\cdot 2E_2}\delta^4(p_1+p_2-p_3-p_4-p_5). \tag{21}$$

We use the notation given by Weber:[21]

$$\sum|T|^2=nm_2N\sum_{L,S}\tilde{R}^2_{LS}(q')\sum_{\lambda_4\lambda_q}|\langle\lambda_4|T_q|\lambda_q\rangle|^2 . \tag{22}$$

The indices refer to the states of the particles as presented in Fig. 2(b).

The single particle probability density is

$$W(q')=\frac{1}{(2\pi)^3}\sum_{LS}\tilde{R}^2_{LS}(q') , \tag{23}$$

in which the primed quantities are in the nuclear system. The factor N takes account of the transformation of the nuclear system to the laboratory system,[21]

$$N=\frac{2J_i+1}{4\pi}\frac{E'_5}{m_5}\frac{E'_q}{m_q} . \tag{24}$$

The T matrix element for the quasifree scattering is obtained from the elementary pion m_q scattering cross section which is known from experiments,

$$\sigma_{\pi q}=\frac{1}{|v_0-v_q|}\int\sum|T_{\pi q}|^2\frac{d^3p_3}{(2\pi)^3 2E_3}\frac{d^3p_4 m_4}{(2\pi)^3 E_4}\times\frac{(2\pi)^4}{2E_0E_q}\delta^4(p_0+q-p_3-p_4) . \tag{25}$$

In this model the scattering is on the mass shell, therefore the incoming pion has four-momentum p_0 and the four-momentum of the fermion m_q, either a proton or a triton, is q.

The quantity n in formula (22) designates the number of substructures in ^{4}He. If m_q is a proton $n=2$, and if m_q is ^{3}H, $n=1$.[20]

The cross sections are derived for the cases in which either the proton or the triton is the transferred particle m_q. These cases can be identified in the experiment. The elementary scattering cross sections for the upper vertex are taken from experiments and they are parametrized for small momentum transfers, which is the case in this experiment. For the (πp) cross section the following parametrization for small t is used:[22]

$$\left[\frac{d\sigma}{dt}\right]_{\pi p}=50e^{8.22t}\ \mathrm{mb/(GeV/}c)^2 . \tag{26}$$

The (πt) cross section has not been measured. However, the (π^4He) cross section was measured by Nomofilov *et al.*[23] According to Glauber's multiple scattering the cross section for single scattering from ^{3}H should be $(\frac{3}{4})^2$ of the cross section for the scattering from ^{4}He. Therefore we use the cross section parametrization:

$$\left[\frac{d\sigma}{dt}\right]_{\pi^3\mathrm{H}}=\frac{9}{16}\left[\frac{d\sigma}{dt}\right]_{\pi^4\mathrm{He}}=310e^{27.9t}\ \mathrm{mb/(GeV/}c)^2 . \tag{27}$$

The probability density is[20]

$$W(q')=N'\left[\frac{1}{\alpha^2+q'^2}-\frac{1}{\beta^2+q'^2}\right]^2,\quad \alpha=(2\mu B_{\mathrm{pt}})^{1/2}=0.846\ \mathrm{fm}^{-1},\quad \beta=1.12\ \mathrm{fm}^{-1} . \tag{28}$$

For the discussion of the results of the calculation we have to review the kinematics of the experiment. The 5 GeV/c quasifree scattered π^- is detected only to the left-hand side in a 3 to 5 GeV/c interval with momentum transfer, $0.005<t<0.15$ (GeV/c)^2. Tritons were detected to the left-hand side as well as to the right-hand side in an angular interval between 45° and 135° and with momentum 0.24 or $0.36\leq p_T\leq 0.6$ GeV/c. The lower limit of 0.24 GeV/c was used as a cut for the momentum distributions of the triton, whereas the limit 0.36 was used for the angular distributions of the triton.

If a triton is observed on the same side as the scattered pion, on the left-hand side, then the majority of the events are of the type triton spectator and the pion scatters from the proton. In this case only events are detected for which the Fermi momentum of the ^{3}He is large (>0.2 GeV/c); the probability density is small and consequently, the cross section will be small. Conversely, if the triton is detected on the right-hand side it has been scattered by the pion to that side and the proton which is not observed is spectator. In that case the pion can scatter from a triton which possesses very little or no Fermi momentum

into the range above 0.3 GeV/c. The observed cross section for the process is as expected an order of magnitude larger than the former one. The density distribution as given by (28) drops rapidly for increasing q'. The calculated cross section turns out to be two orders of magnitude larger than for the scattering of the triton to the left-hand side. This type of calculation does not take into consideration the fact that the final state has to be orthogonal to the initial state. Fujita and Hüfner[24] showed that this condition may reduce the cross section by an order of magnitude. They derived a function for this "orthogonality defect" for the fragmentation of ^{4}He. Therefore, their parametrized function is directly applicable. Since the Fujita-Hüfner formula reduced the cross section by too large a factor, another inhibition factor was tried which derives from the occupation of states in a Fermi gas model

$$C=1-\frac{W(q)q^2dq}{2\frac{4\pi}{(2\pi)^3}q^2dq\,V}, \tag{29}$$

where $W(q)$ is the density of states as given by formula (28) and V is the nuclear volume in fm^3. Since complete occupation of all states may be at $q=0$, V is set by this condition. For $V=4\pi r_0^3A/3$, the radius r_0 is slightly larger than normal (about 1.6 fm).

Fäldt[20] assumed that the probability of finding ^{3}H in a ^{4}He is about 0.8. This is in accordance with estimates by Greben.[25] The same factor is used in the present calculations.

For the presentation and the comparison with the data, the calculated cross sections have to be integrated over the experimentally observed ranges. The variables for the calculation are the magnitude of the Fermi momentum, its angle with respect to the incoming particle, and the scattering angle in the upper vertex. In principle, an analytical calculation of the Jacobian for the transformation of these variables to the experimental variables is possible. However, since the equations become rather complicated we used a constant interval stepping for the internal variables and added the cross sections in each experimental bin. The calculated cross section in a bin is then the summed value over the number of times each bin has been entered. Both the intervals of the stepping and the bin size were changed for a check on the quality of the method. The presented curves are drawn through the center between two bins. As in Ref. 19 the theoretical cuts do not agree precisely with the experimental cuts.

Two groups of curves are shown each for the right scattered and for the left scattered triton. As mentioned before, the right scattered triton is the result of the π^- being quasifree scattered from the triton, where the proton is the spectator, whereas for the left scattered triton the triton is the spectator.

Figures 4(a) and (b) show the momentum distribution of the triton for both sides. The drawn curves are for the Pauli blocking in the plane wave approximation, the dotted curve is obtained by making use of the Fujita-Hüfner function. In Fig. 4(b), for the left scattered triton the dash-dotted line shows a contribution from pions quasielastically scattered from the triton. The latter reac-

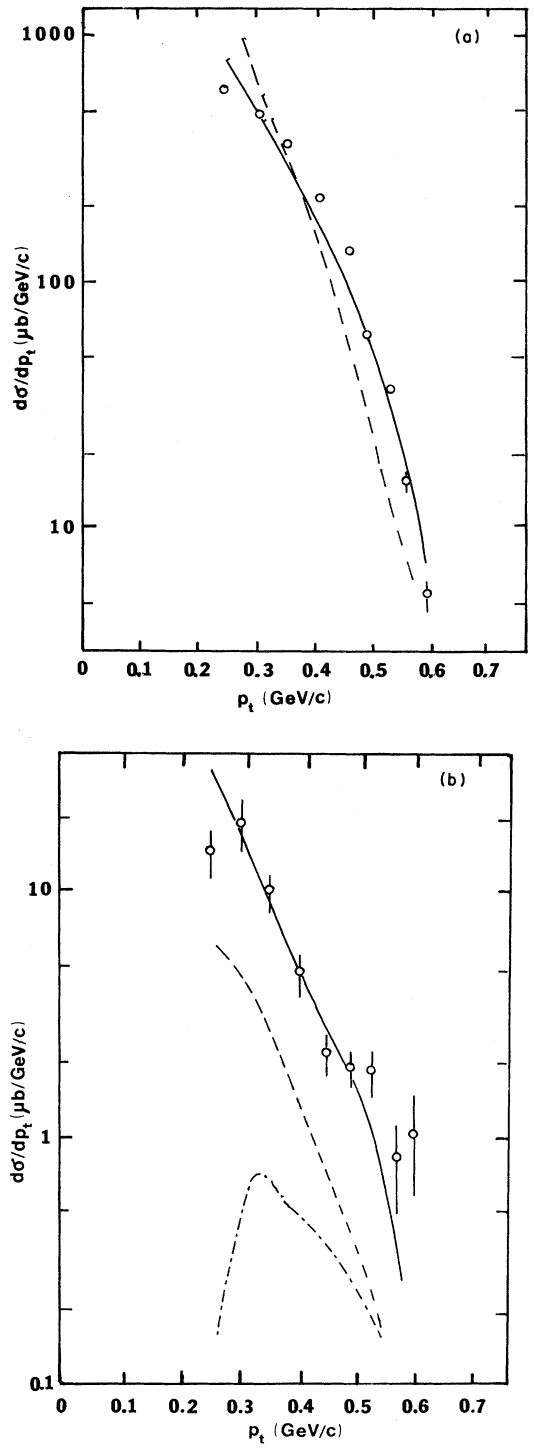

FIG. 4. (a) The reaction ^{4}He(π^-,π^-p)^{3}H. The momentum distribution of right scattered tritons (Refs. 19 and 20). The full curve is the result of the present calculation and Pauli blocking of formula (29). The dashed curve is the result with the Pauli blocking of Ref. 24. The cuts in all figures are the same as in Ref. 19. (b) The momentum distribution of left scattered tritons. The full and dashed curves have the same meaning as in (a). The dot-dashed curve is the result of a calculation in which the proton is the spectator possessing such large Fermi momentum to the right that it can balance the momentum of the pion and the triton to the left.

tion is possible only when the triton possesses very large Fermi momentum. Its contribution consequently is more than one order of magnitude down.

Figures 5(a) and (b) show the angular distribution of the triton. The Pauli blocking reduces for right scattered tritons the cross section by a factor of 10. However, it seems that for these tritons the assumed inhibition is slightly too large, so that a dip shows at the peak position. A very small change in the amount of blocking would increase the cross section to the experimental points at $\cos\theta_t=0.1$ and $\cos\theta_t=0.2$ for which q is close to zero momentum without changing the other parts of the curve appreciably. The Fujita-Hüfner formula reduces the cross section by more than a factor of 10. Unfortunately, the triton momentum cut in the momentum distribution is not the same as the cut in the angular distribution measurement.

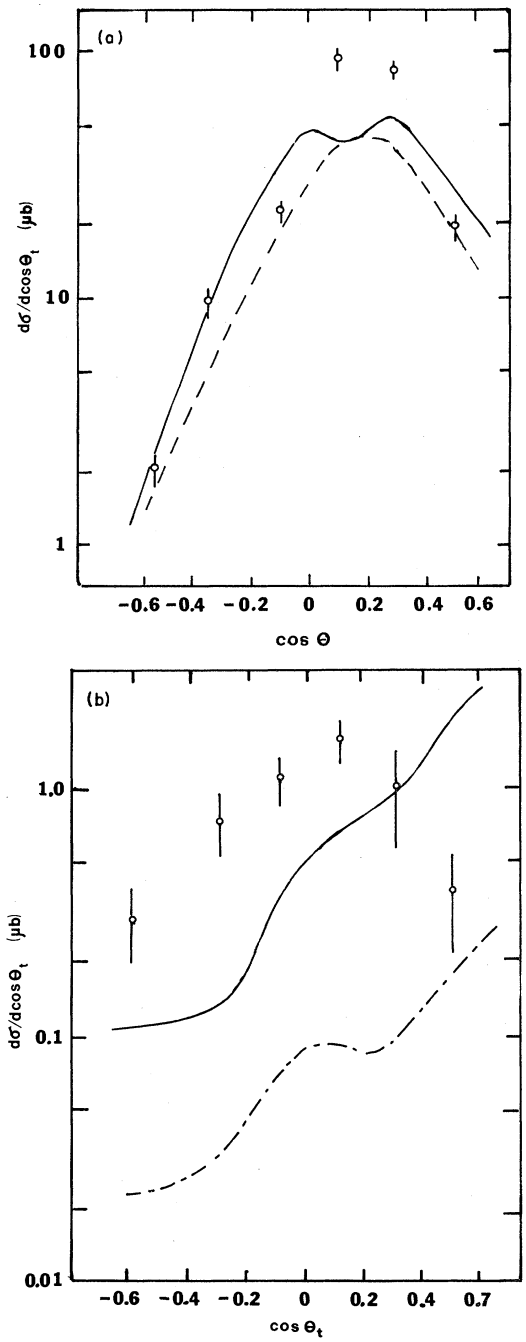

FIG. 5. (a) The angular distribution of tritons scattered to the right from the reaction $^4\mathrm{He}(\pi^-,\pi^-\mathrm{p})^3\mathrm{H}$. Both curves have the same meaning as in Fig. 4(a). The Pauli blocking of formula (29) is too much for small Fermi momentum. (b) The angular distribution of tritons scattered to the left. The meanings of the curves are the same as in Fig. 4(b). In this case the Pauli blocking of Ref. 24 reduces the cross section by more than an order of magnitude and it is not shown.

Figure 5(b) shows the least agreement with the experimental data. Since the single scattering cross section is small it is possible that contributions from double scattering become important. The pion would scatter first from a proton and afterwards from the triton. Simple kinematics show that the cross section would peak at about $\theta_t=90°$. A very approximate estimate yields a cross section which is of the same order as that for the single scattering. The double scattering amplitude would interfere with the single scattering. Such a calculation, however, is beyond the present model. The Fujita-Hüfner blocking reduced the cross section by an order of magnitude and therefore it is not shown in Fig. 5(b). An additive interference between the two curves of Fig. 5(b) would result in better agreement with the first four experimental points. However, the present calculation does not contain any phase information.

Except for the curves in Fig. 5(b), the fits are as good as those obtained by Chevallier *et al.*[19] Also, these authors remark that a simple impulse approximation is not able to give any result which resembles the data. This calculation is much less elaborate and more accessible to any variation in parameters.

V. CONCLUSIONS

The examples presented above which are all hadron induced reactions are in good agreement with experiments. The correction proposed by this model is only kinematical. Distortions, multiple scattering, and the propagation of incident or produced particles through the nuclear medium have to be considered in addition. The scattering matrix should be taken inside the medium. This model, however, used a scattering amplitude which is on shell. Unless this amplitude changes rapidly with energy the model is very effective in predicting the peak position of quasielastic scattering. It is unlikely that distortions will shift the peak position in momentum spectra. They will decrease the cross section by a slowly varying function of the momentum. However, double scattering may induce peaks or valleys as a consequence of phase relations between amplitudes which are difficult to incorporate in a model as simple as the one presented here.

Lepton induced reactions may have to be discussed separately. Moniz *et al.*[8] discuss the observed shifts of the peak position which increase with decreasing scattered-electron energy. For a Fermi gas model excellent agreement has been obtained with the data of Refs. 8 and 26. However, the Fermi momentum width and the separation energy are free parameters. The latter is about

20 MeV for light elements and about 40 MeV for heavy elements.

The present model with the proper binding energy of the proton and zero Fermi momentum calculates the peak position at 0.384 GeV/c instead of about 0.375 GeV/c experimentally. This discrepancy could be due to a small error in the incident or scattered electron energy. However, the shift is A dependent to a greater amount than the present model would predict. Rosenfelder[27] attributes the shift to the exchange parts of the two-body interaction. In a local ordinary optical potential bound state and continuum state interactions seem to cancel completely. The binding energy correction should apply. One may have to consider that the electron nucleon interaction consists of two contributions, the longitudinal or Coulomb part, and the transverse part or current interaction. Therefore, one cannot assume that the peak position corresponds only to zero Fermi momentum. The shifts can be explained by the introduction of a small amount of Fermi momentum which for ^{12}C is only 50 MeV/c. This is actually less than one would expect from the peak position in the density distribution of the p-wave proton. But it is more reasonable than the large energies used in Ref. 8.

Unfortunately, more data and more extensive calculations will be necessary for a better understanding of the cause of the shift in lepton induced reactions. Even worse is the situation for pion production experiments. The large momentum mismatch in such reactions makes one believe that simple quasifree reaction interpretations are not appropriate and that triangle diagrams will be required to fit the data. Some attempts in this direction seemed promising. This model makes possible on-shell calculations in triangle diagrams.

At present we can conclude that the model gives good fits for hadron induced quasifree reactions at incident energies above 100 MeV. The calculations of the cross sections are so simple that they can be carried out on small computers. The applicability of the model for lepton induced reactions is not yet completely understood.

ACKNOWLEDGMENTS

The author is grateful for the hospitality of the Max-Planck-Institut für Kernphysik at Heidelberg and especially for the hospitality and interest of Professor B. Povh. Professor H. J. Weber and Professor J. Hüfner have contributed much to this model and I am grateful for their interest and help. The author would also like to thank the Alexander von Humboldt Foundation for the presentation of the Senior Award.

*On leave from the University of Virginia, Charlottesville, VA 22901.

[1]T. Berggren and H. Tyren, Annu. Rev. Nucl. Sci. **16**, 353 (1965); G. Jacob and Th. A. J. Maris, Rev. Mod. Phys. **45**, 6 (1973).

[2]I. M. Narodetsky, Yu. A. Simonov, and F. Palumbo, Phys. Lett. **58B**, 125 (1975); J. M. Eisenberg, J. V. Noble, and H. J. Weber, Phys. Rev. C **19**, 276 (1979).

[3]F. Lenz, Ann. Phys. (N.Y.) **108**, 116 (1977).

[4]Y. Horikawa, M. Thies, and F. Lenz, Nucl. Phys. **A345**, 386 (1980).

[5]M. Thies, Nucl. Phys. **A382**, 434 (1982).

[6]C. H. Q. Ingram *et al.*, Phys. Rev. C **27**, 1578 (1983).

[7]R. E. Chrien, T. J. Krieger, R. J. Sutter, M. May, H. Palevsky, R. L. Stearns, T. Kozlowski, and T. Bauer, Phys. Rev. C **21**, 1044 (1980).

[8]E.g., E. J. Moniz, I. Sick, R. R. Whitney, J. R. Ficenec, R. D. Kephart, and W. P. Trower, Phys. Rev. Lett. **26**, 445 (1971).

[9]A. Abul-Magd, J. Hüfner, and B. Schürmann, Phys. Lett. **60B**, 327 (1976).

[10]E. F. Redish, Phys. Rev. Lett. **31**, 617 (1973).

[11]E.g., R. Hagedorn, *Relativistic Kinematics* (Benjamin, New York, 1963).

[12]S. B. Treiman and C. N. Yang, Phys. Rev. Lett. **8**, 14 (1962).

[13]S. N. Bunker, M. Jain, C. A. Miller, J. M. Nelson, and W. T. H. van Oers, Phys. Rev. C **12**, 1396 (1975).

[14]M. Jain, P. G. Ross, H. G. Pugh, and H. D. Holmgren, Nucl. Phys. **A153**, 49 (1970).

[15]R. Minehart *et al.* (private communication).

[16]S. Frankel, W. Fraiti, C. F. Perdrisat, and O. B. van Dyck, Phys. Rev. C **24**, 2684 (1981).

[17]H. J. Weber and L. D. Miller, Phys. Rev. C **16**, 726 (1977).

[18]S. Jonsson *et al.*, Phys. Rev. C **21**, 306 (1980).

[19]M. Chevallier *et al.*, Nucl. Phys. **A343**, 449 (1980).

[20]G. Fäldt, Phys. Scr. **23**, 215 (1981).

[21]H. J. Weber (private communication).

[22]Particle Data Group, National Standard Reference Data System, Lawrence Berkeley Laboratory Report No. LBL-63, 1973.

[23]A. A. Nomofilov *et al.*, Yad. Fiz. **18**, 364 (1973) [Sov. J. Nucl. Phys. **18**, 187 (1974)].

[24]T. Fujita and J. Hüfner, Nucl. Phys. **A343**, 493 (1980).

[25]J. M. Greben, Phys. Lett. **115B**, 363 (1982).

[26]R. R. Whitney, I. Sick, J. F. Ficenec, R. D. Kephart, and W. P. Trower, Phys. Rev. C **9**, 2230 (1974).

[27]R. Rosenfelder, Ann. Phys. (N.Y.) **128**, 188 (1980).